J. Chem. Soc., Faraday Trans. 2, 1989, **85**(9), 1447–1463

Reaction of H Atoms with some Silanes and Disilanes

Rate Constants and Arrhenius Parameters

Neville L. Arthur,† Peter Potzinger,*‡ Bruno Reimann§ and H. Peter Steenbergen

Max-Planck-Institut für Strahlenchemie, Stiftstrasse 34–36, 4330 Mülheim a.d. Ruhr, Federal Republic of Germany

Arrhenius parameters have been measured for H abstraction by H atoms from the Si—H bond in a number of differently substituted silanes and disilanes. In the case of silane and trimethylsilane kinetic isotope effects have also been determined. The available data on the reactions studied are collated and evaluated, and the trends which emerge are discussed.

The kinetics of the gas-phase reactions of atoms and free radicals with silanes have been extensively studied.[1] Attack by the H atom, the simplest free-radical species, is of particular interest: kinetic parameters for H-atom reactions provide an uncomplicated probe of chemical reactivity; attack on silanes can be contrasted with the large body of literature for H-atom attack on other substrates;[2] in the case of the simpler silanes, Arrhenius parameters and kinetic isotope effects can be compared with the results of calculations based on semiempirical models,[3,4] allowing some insight into the nature of the reaction path.

Rate constants for the reactions of H atoms with silanes have been measured in several laboratories,[5–22] Unfortunately, agreement between the results obtained is less than satisfactory, obscuring possible trends which might be expected to emerge for homologous series of substrates. This conflict between results often appears to be associated with the different experimental methods employed. Another deficiency in the data available at present is that most work has been carried out only at room temperature, and therefore few Arrhenius parameters have been reported.

Our objective in embarking on the present work was to make a systematic survey of H-atom attack on silanes and disilanes by means of a method which would allow rate constants to be determined over a range of temperatures. Most previous studies have involved the use of the discharge-flow and competitive static photolysis techniques, with their attendant disadvantages: in the former, wall reactions frequently intrude, while in the latter, only relative rate constants can be measured, and the mechanism is not always sufficiently well known for them to be determined unambiguously.

We chose instead to employ a pulsed photolysis approach, with H atoms produced by Hg-sensitized photolysis of H_2, and monitored by Lyman-α absorption. In this paper we describe the apparatus and its operation, and we report results for H-atom attack on the Si—H bond in a number of silanes and disilanes. We also present data for a well characterized test reaction, the addition of H atoms to C_2H_4. Trends in the rate constants, Arrhenius parameters and kinetic isotope effects obtained are discussed, and comparisons are made with previous values in the literature.

† Permanent address: Chemistry Department, La Trobe University, Melbourne, Victoria, Australia 3083.

‡ Present address: Max-Planck-Institut für Strömungsforschung, Bunsenstrasse 10, 3400 Göttingen, Federal Republic of Germany.

§ Present address: Messer Griesheim GmbH, Postfach 4709, D-4040 Düsseldorf, Federal Republic of Germany.

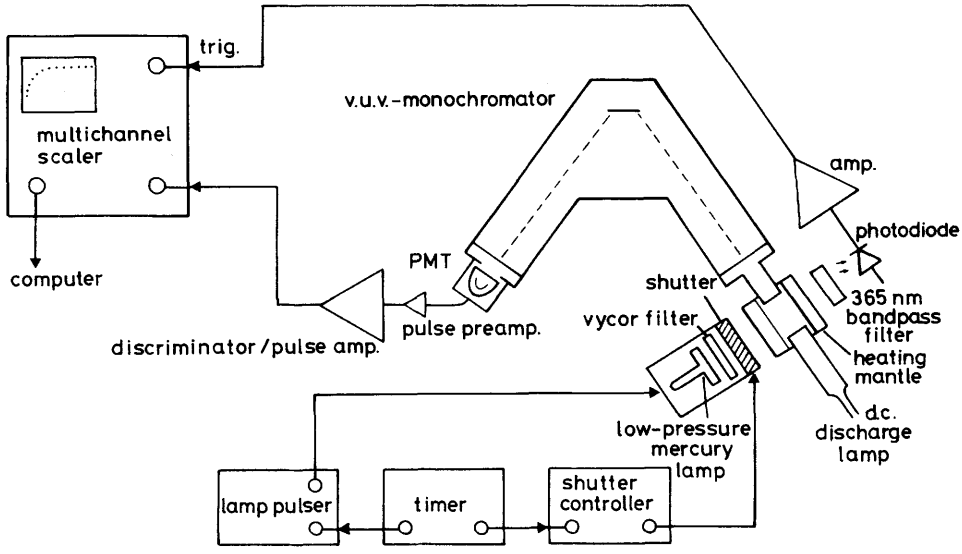

Fig. 1. Overall diagramatic view of apparatus.

Experimental

General Description of the Apparatus

The pulsed photolysis–resonance absorption system is shown diagrammatically in fig. 1. H atoms are generated in a thermostatted quartz cell by Hg-sensitized photolysis of H_2 with 253.7 nm light from a pulsed low-pressure mercury arc lamp. The time-dependence of the concentration of H atoms is followed by measuring the absorption of resonance radiation from a Lyman-α lamp arranged at 90° to the photolysis lamp. After having passed through the cell the 121.6 nm Lyman-α line is isolated by a vacuum-ultraviolet monochromator (0.5 m McPherson 235) and detected by a solar blind photomultiplier (EMR 641 G). The signal from this passes through a pulse amplifier–discriminator (Ortec–Brookdeal) and is then fed to a signal-averaging system (Nicolet 1072 N). The detection and photon-counting system is triggered by the trailing edge of the photolysis light pulse *via* a photodiode. After accumulation, the data are transferred to a main-frame computer and analysed by a non-linear least-squares procedure.

Reaction Cell and Flow System

The quartz reaction cell, a flat cylinder in shape, 1 cm thick and with 5 cm diameter windows, is connected to a slow-flow system. Two diametrically opposed 29 mm sockets allow easy connection to the Lyman-α lamp and to the monochromator, both of which are fitted with MgF_2 windows. The cell is heated by a thermostatted split aluminium block (up to 600 K), and the temperature of the reaction mixture is measured directly by a thermocouple which enters the cell through a narrow side-arm. The reactants, typically 100 kPa H_2 or H_2/He mixture and 1–10 Pa substrate, are mixed and stored in a 20 dm^3 bulb. The pressure of the substrate is measured by an MKS 310BH capacitance manometer, and the total pressure by an MKS 223AH manometer. The reaction mixture is pumped slowly over a drop of Hg in a thermostatted reservoir and thence through the cell, the flow rate being adjusted so that a fresh mixture is exposed to each photolytic

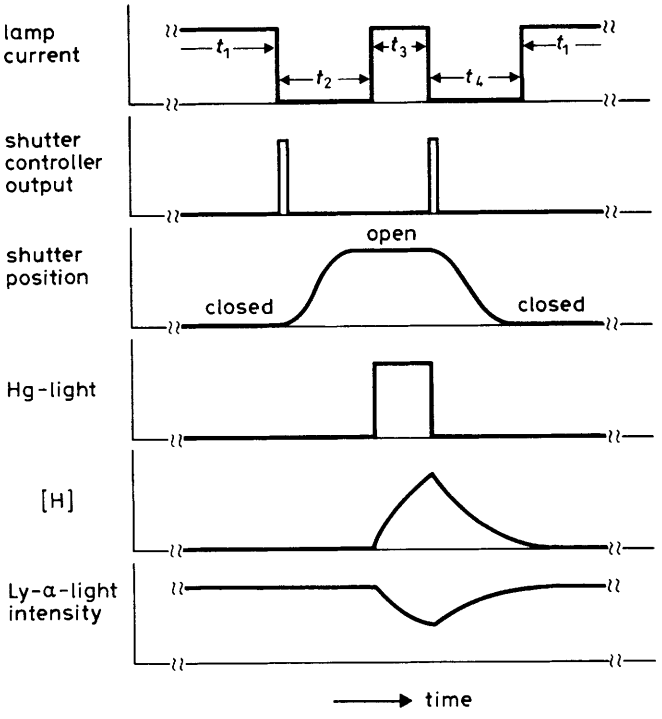

Fig. 2. Operation of the shutter system.

pulse. The pressure in the cell, usually 67 kPa, is held constant by an MKS 250A pressure/flow controller in conjunction with an MKS 251-50 flow valve.

Hg Photolysis Lamp and Shutter System

Hg resonance radiation is produced by a low-pressure Hg lamp (Gräntzel Type 5), thermostatted at 315 K, flushed with nitrogen, and operated at 650 V and 100 mA. 184.9 nm radiation is removed by a Vycor filter. Highly reproducible rectangular light pulses with a repetition frequency of 0.1–1 s^{-1}, are obtained by means of an electrically operated mechanical shutter (Compur M3) in combination with the switching of the lamp, as shown diagrammatically in fig. 2. This arrangement is necessary because the mechanical shutter alone, with an opening and closing time of 3 ms, is too slow for the kinetics to be observed, while merely switching the lamp on and off leads to poor reproducibility as a result of cooling in the long dark periods between pulses. The operation of the shutter and the lamp is controlled by a timer based on a 1 MHz quartz crystal oscillator.

The light pulses produced show a rise and fall time of *ca.* 30 μs (10%–90% signal height) which should allow pseudo-first-order rate constants up to 3×10^3 s^{-1} to be measured. In practice, however, rate constants up to only 10^3 s^{-1} can be measured within an experimental time of *ca.* 1 h because of the limitations imposed on the accumulation of data by the Lyman-α count rate (*ca.* 2×10^5 s^{-1}) and the photon-counting method.

The absorbed photolysis light intensity, I_{abs}, typically 5×10^{14} s^{-1} cm^{-3}, was determined either by propane actinometry[23] or by measuring the *cis–trans* isomerization of but-2-ene.[24] It was varied by either changing t_3 (fig. 2), or by interposing wire meshes,

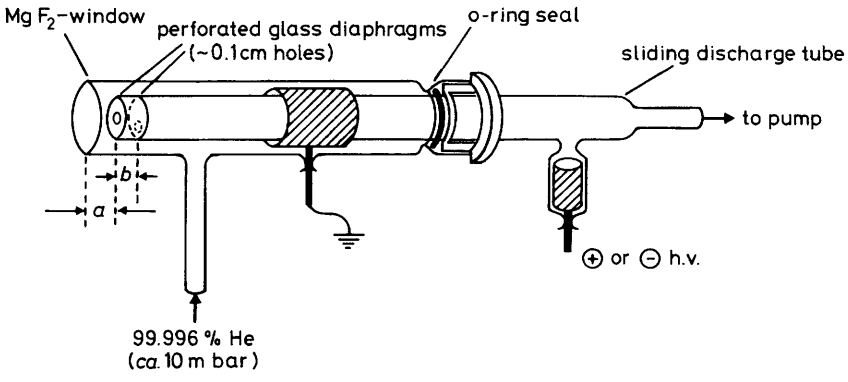

Fig. 3. Lyman-α lamp.

the transmission of which was found by actinometry to be given by $(0.48)^n$, where n is the number of meshes.

Lyman-α Lamp

The Lyman-α lamp, which follows the design of Lifshitz *et al.*,[25] is of the glow-discharge type, and is shown in fig. 3. The thickness of the emitting layer $(a+b)$ can be continuously varied by altering the distance a, but in practice $(a+b)$ is usually *ca.* 1 cm. At this distance the plasma touches the MgF_2 window, and this, together with the very small concentration of H_2 in the He used (He > 99.996%), ensures that the effect of self-absorption on the output of the lamp is minimal.

H-atom Generation by Hg-resonance Absorption

The Hg-sensitized photolysis of H_2 is well known as a clean source of thermal H atoms.[26] Since they are produced in a resonance absorption process, however, they are not generated uniformly throughout the cell but show a concentration gradient across it. We have estimated this gradient in the following way.

The 253.7 nm Hg resonance transition consists of 10 closely spaced hyperfine lines.[27] In emission, the lines, although Doppler-broadened at the temperature of the Hg atoms in the lamp (*ca.* 600 K), and flattened by self-absorption, are still separated. In absorption, on the other hand, the lines are each subject to strong pressure broadening, and overlap to form a single broad absorption band. This suggests that the absorption of Hg resonance light is likely to follow Beer–Lambert behaviour, and this was confirmed by measuring the absorbance of Hg in 67 kPa of He in cells of different pathlength. The value of the effective cross-section obtained was $\sigma_{\text{eff}} = 1.3 \times 10^{-14}$ cm^2. This value is in agreement with previously published values, and is an order of magnitude smaller than the value measured in the absence of pressure broadening.[26] Substituting I_{abs} and σ_{eff} into the Beer–Lambert law shows that the H-atom concentration from window to window across the cell differs by a factor of *ca.* 2.

We have investigated the influence of the resulting H-atom concentration gradient on the pseudo-first-order rate constant by numerical solution of the diffusion equation, assuming that H atoms are lost only at the wall and that all H atoms striking the wall are lost. The calculation shows that after an initial 20 ms period of disorder, the system settles and becomes first-order, with a rate constant $k_w = 35\ \text{s}^{-1}$. This value is a factor of 2 higher than the experimentally observed rate constant, indicating that some H atoms striking the wall are not lost there, *i.e.* that the loss of H atoms is determined not

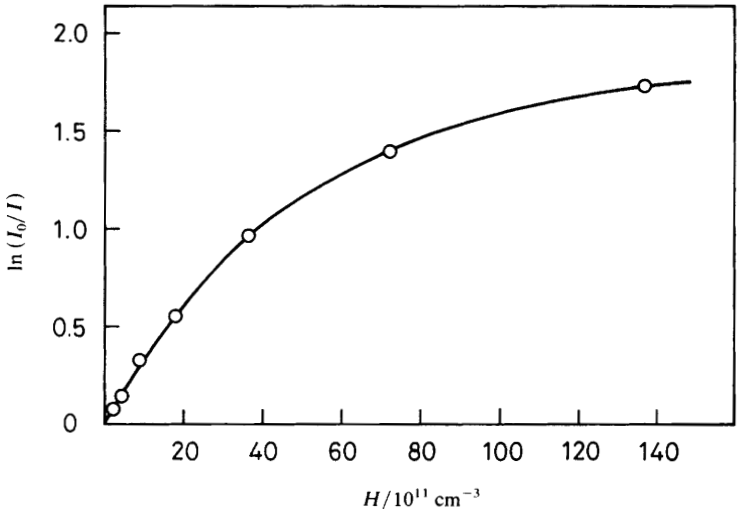

Fig. 4. Absorbance as a function of [H].

only by diffusion to the wall, but also by the activity of the wall. This effect can be expressed in quantitative terms by γ, the 'sticking coefficient',[28] for which a value of 2×10^{-4} is required to reproduce the measured value of k_w. This is a reasonable value for an untreated quartz surface.

Lyman-α Resonance Absorption

Since in line absorption there is no simple linear relationship between absorbance and concentration, it was necessary to establish a calibration curve relating Lyman-α absorption and the H-atom concentration.

The mechanism of the Hg-sensitized photolysis of H_2 has been well authenticated and consists of the following reactions:[29]

$$\mathrm{Hg} \overset{h\nu}{\rightleftharpoons} \mathrm{Hg^*} \quad (1)$$

$$\mathrm{Hg^* + H_2} \longrightarrow \mathrm{Hg + 2H} \quad (2)$$

$$\longrightarrow \mathrm{HgH + H} \quad (3)$$

$$\mathrm{H + HgH} \longrightarrow \mathrm{H_2 + Hg} \quad (4)$$

$$\mathrm{HgH + M} \longrightarrow \mathrm{Hg + H + M} \quad (5)$$

$$\mathrm{2H + M} \longrightarrow \mathrm{H_2 + M} \quad (6)$$

$$\mathrm{H} \longrightarrow \mathrm{H_w}. \quad (7)$$

From this it can be seen that to a first approximation the maximum concentration of H atoms, at the end of the light pulse, is equivalent to $2I_{abs}$, where I_{abs} is the absorbed light intensity. The H-atom concentration can be estimated more exactly, however, by integrating the coupled differential equations corresponding to the various steps of the mechanism. The H-atom concentration calculated in this way at various absorbance values following a 20 ms light pulse attenuated by a variable number of wire meshes, is shown in fig. 4. In order to obtain a functional relation between absorbance and the H-atom concentration, c, values of P and Q in the empirical two-parameter equation

$$\ln(I_0/I) = P[1-\exp(-Qc)] \quad (8)$$

were found by fitting it to the points in fig. 4 by means of a non-linear least-squares procedure. From the slope of this curve at small H-atom concentration the absorption cross-section for H atoms can be calculated, the value obtained being $\sigma(H) = 8 \times 10^{-14}$ cm^2. As with σ_{eff} for the absorption of Hg atoms, $\sigma(H)$ is also an order of magnitude lower than the theoretical value, in this case calculated assuming a linewidth appropriate to our experiment, $\Delta\bar{\nu} = 1$ cm^{-1}, and an oscillator strength of 0.8324.[30]

If c is assumed to follow simple first-order decay, the time dependence of the transmitted Lyman-α radiation is given by

$$I(t) = I_0 \exp(-P\{1 - \exp[-Qc_0 \exp(-k^1 t)]\}) \quad (9)$$

where k^1 is the pseudo-first-order decay constant. This function is fitted to our experimental time-dependent Lyman-α intensity data with I_0, c_0 and k^1 as adjustable parameters.

Materials

Most of the substrates were of commercial origin. Their purities were checked by gas chromatography and mass spectrometry, and where necessary, they were purified by preparative gas chromatography. Monochlorosilane was prepared as described by Stock and Somieski;[31] mass-spectrometric analysis revealed the presence of 0.3% dichlorosilane. Trifluorosilane was prepared by a modification of the method of Booth and Stillwell,[32] in which SbF_3 was dropped into liquid trichlorosilane containing $SbCl_5$, the gas evolved being purified by trap-to-trap distillation. [$^2H_4$]Silane and [$^2H_1$]trimethylsilane were prepared by reducing the corresponding chlorosilanes with $LiAlD_4$.[33]

Results

Reaction of H Atoms with Silanes and Disilanes

Typical transmitted Lyman-α intensity data as a function of time, in this case for $H + (CH_3)_2SiH_2$, are illustrated in fig. 5. Apparent first-order rate constants, k^1, were extracted from such data by the procedure outlined in the previous section. For all of the reactions studied, it was found that k^1 depended on the absorbed intensity of the photolysing light, I_{abs}, in a characteristic way. This is shown for $H + (CH_3)_2SiH_2$ in fig. 6, from which it can be seen that k^1 decreases as I_{abs} is reduced, and that the extrapolated value at $I_{abs} = 0$ is close to 1/2 of the limiting value at high I_{abs}. This pattern of behaviour is to be expected if the radicals formed by H-atom atack on the substrate not only combine with each other, but also with H atoms:

$$H + RH \rightarrow H_2 + R \quad (10)$$

$$H + R \rightarrow RH \quad (11)$$

$$2R \rightarrow R_2 \quad (12)$$

$$H \rightarrow H_w \quad (7)$$

Application of the steady-state treatment to R shows that at high I_{abs}, where reaction (11) predominates, $k^1 = 2k_{10}[RH]$, whereas at low I_{abs}, where reaction (11) is negligible, $k^1 = k_{10}[RH]$, *i.e.* half the value at high I_{abs}. We consider the value of k^1 extrapolated to $I_{abs} = 0$ to be the true first-order rate constant for the reaction of H atoms with a substrate. The problem of the dependence of k^1 on I_{abs} could be avoided by the use of high substrate concentrations, but this course of action is not feasible because it would result in an unacceptable loss of transmitted Lyman-α intensity.

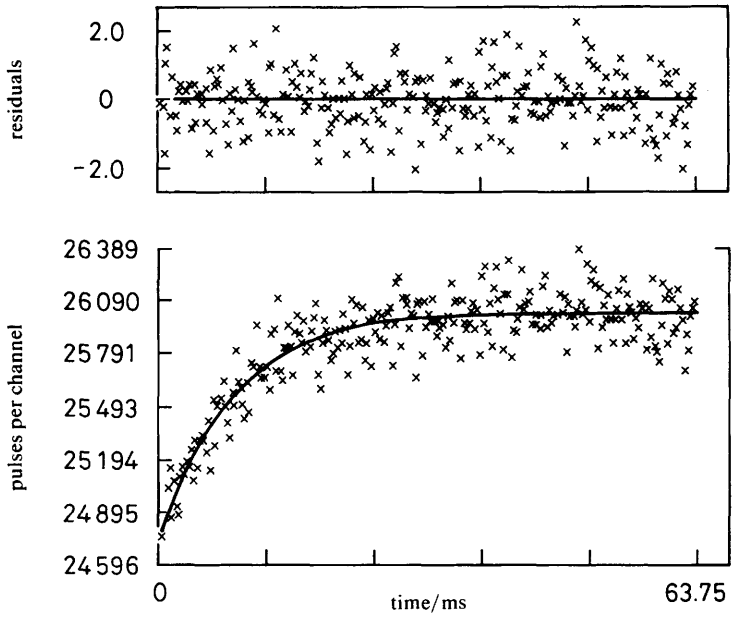

Fig. 5. Typical Lyman-α light intensity at the detector as a function of time for the reaction $H+(CH_3)_2SiH_2$. $[(CH_3)_2SiH_2] = 3.1\times10^{13}$ cm^{-3}, $t_3 = 0.13$ ms.

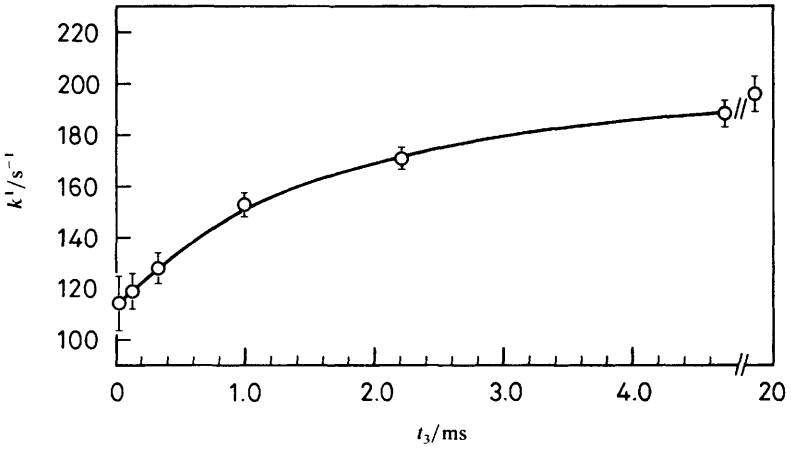

Fig. 6. Dependence of k^1 on t_3. The absorbed intensity per light pulse I_p is taken to be proportional to t_3, $I_p \approx 5\times10^{11}\times t_3$ cm^{-3}. $[(CH_3)_2SiH_2] = 3.1\times10^{13}$ cm^{-3}.

Using this mechanism, we have also simulated the dependence of k^1 on I_{abs} by computer calculations, and in all cases found that the values $k_{11} = (1\text{-}3)\times10^{-10}$ cm^3 s^{-1} and $k_{12} \leq 5\times10^{-11}$ cm^3 s^{-1} satisfactorily reproduce the experimental results. Other reactions may be involved in some cases, but a more elaborate mechanism could not be considered owing to lack of data, and in any case this seemed unwarranted since the simple mechanism adequately accounted for the observed experimental behaviour.

For each substrate, extrapolated k^1 *values*, k_0^1, were determined at room temperature over a range of substrate concentrations, and the bimolecular rate constant, k_{10}, was

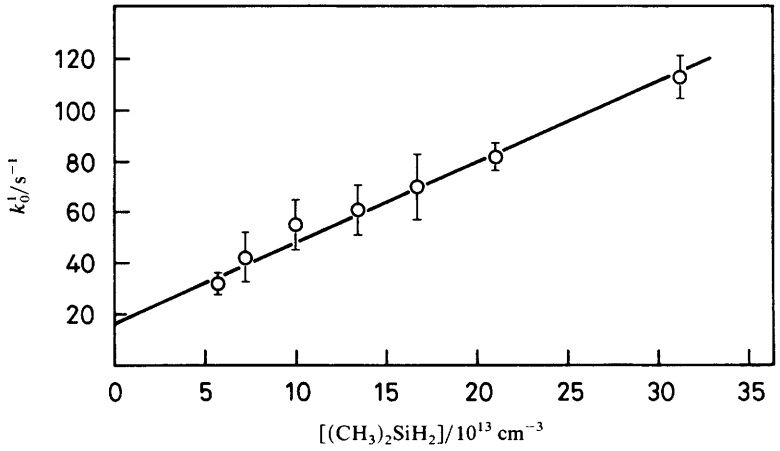

Fig. 7. Plot of k_0^1 *versus* $[(CH_3)_2SiH_2]$ at room temperature.

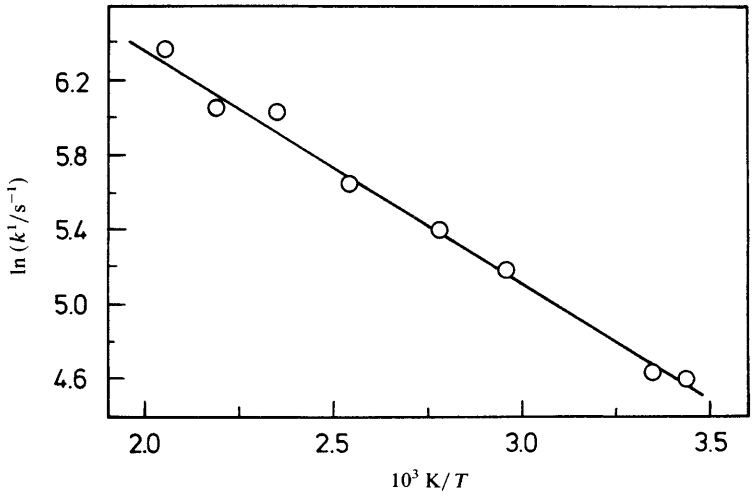

Fig. 8. Arrhenius plot of k^1 for $H+(CH_3)_2SiH_2$.

then evaluated from the slope of a plot of k_0^1 *versus* [substrate]. A typical plot, for $H+(CH_3)_2SiH_2$, is shown in fig. 7.

The temperature dependence of k^1 was studied at only one intensity, a medium value corresponding to $t_3 = 1.3$ ms, which represented a compromise between keeping the H-atom concentration as low as possible, and an acceptable expenditure of time. A typical Arrhenius plot of k^1 is given in fig. 8 for $(CH_3)_2SiH_2$. Computer simulation showed, however, that a systematic error was introduced by not extrapolating the k^1 values to $I_{abs} = 0$, and it was therefore necessary to correct the experimental activation energy for this effect. The procedure involved first fitting values of k^1, computed on the basis of the above mechanism, to the corresponding experimental room-temperature k^1 *versus* I_{abs} data; k_{10} was taken to be the extrapolated zero intensity value, k_w was taken from the relevant plot of k^1 *versus* [substrate], and k_{11} and k_{12} were varied until a good fit was obtained. These values of k_{11} and k_{12}, assumed to be temperature independent, were then used, together with the appropriate value of k_w, and a k_{10} value

Table 1. Pulsed photolysis results for the reactions of H atoms with silanes and disilanes

	T/K^a	$(E_a/R)/K$	$A/10^{-11}$ cm^3 s^{-1}	$k_0/10^{-13}$ cm^3 s^{-1}	$(E_a/R)_0/K$	$A_0/10^{-11}$ cm^3 s^{-1}
SiH_4	294–487	1332 ± 14	2.9 ± 0.1	2.0 ± 0.1	1400 ± 37	2.3 ± 0.3
SiD_4	292–494	1667 ± 12	3.4 ± 0.1	0.85 ± 0.04	1830 ± 83	4.2 ± 1.2
CH_3SiH_3	291–489	1216 ± 28	3.4 ± 0.3	4.0 ± 0.1	1360 ± 79	4.0 ± 1.1
$(CH_3)_2SiH_2$	292–489	1233 ± 23	3.3 ± 0.2	3.1 ± 0.1	1406 ± 90	3.6 ± 1.1
$(CH_3)_3SiH$	290–485	1112 ± 32	1.8 ± 0.2	2.6 ± 0.1	1230 ± 69	1.7 ± 0.4
$(CH_3)_3SiD$	292–500	1412 ± 8	1.4 ± 0.03	0.66 ± 0.02	1615 ± 102	1.6 ± 0.6
$(C_2H_5)_3SiH$	294–486	1058 ± 16	1.75 ± 0.08	3.1 ± 0.3	1110 ± 31	1.3 ± 0.2
SiH_3Cl	289–483	1418 ± 23	3.1 ± 0.2	1.7 ± 0.1	1526 ± 62	3.0 ± 0.4
SiH_2Cl_2	290–493	1459 ± 19	2.1 ± 0.1	1.1 ± 0.1	1614 ± 80	2.5 ± 0.7
$SiHCl_3$	290–482	1111 ± 24	0.27 ± 0.02	0.53 ± 0.04	1280 ± 88	0.41 ± 0.13
$C_6H_5SiH_3$	290–485	1285 ± 21	3.8 ± 0.3	4.9 ± 0.2	1450 ± 96	6.7 ± 2.0
Si_2H_6[b]	294–408	1155 ± 25	7.0 ± 0.6	12.9 ± 1.8	1326 ± 104	11.6 ± 4.4
$(CH_3)_5Si_2H$[b]	293–409	967 ± 41	2.7 ± 0.5	10.3 ± 0.4	996 ± 45	3.0 ± 0.5

[a] Temperature range over which k^1 was measured. [b] Original experimental data from ref. (22).

Table 2. Room-temperature[a] rate constants for H- and D-atom attack on silanes and disilanes

experimental system[b]	$k/10^{-13}$ cm^3 s^{-1}	ref.
	H + SiH_4	
H_2-Hgp/s/Lα, ref. C_2H_2	13 ± 4[c]	6
H_2-d/f/ms	>2.2	5
H_2-d/f/ms	26 ± 3	9
H_2-d/f/Lα	85 ± 7	10
H_2-pr/s/Lα	2.3 ± 0.3[d]	17
H_2-Hgp/s/ms, ref. C_2H_4	2.2 ± 0.3[d]	11
H_2-d/f/ms	4.4 ± 0.7	20
H_2-Hgfp/sf/Lα	2.0 ± 0.1	this work
	D + SiH_4	
C_2D_4-p/s/ref. C_2D_4	2.5 ± 0.6[e]	7
D_2-pr/s/Lα	1.9 ± 0.4	17
C_2D_4-p/s/ref. C_2D_4	2.0 ± 0.5[e]	14
D_2-d/f/esr	3.0 ± 1.0	15
D_2-d/f/ms	3.0 ± 0.7	9
D_2-d/f/ms	3.9 ± 0.7	20
	H + SiD_4	
C_2H_4-p/s/ref. C_2H_4	1.4 ± 0.1[d]	14
HI-p/s/ref. HI	≤3.0	16
H_2-Hgp/s/m, ref. C_2H_4	0.79 ± 0.07[d]	11
H_2-Hgfp/sf/Lα	0.85 ± 0.04	this work
	H + CH_3SiH_3	
H_2-Hgp/s/Lα, ref. C_2H_2	7.8 ± 2.6[c]	6
H_2-d/f/ms	11.5 ± 2.0	9
H_2-Hgp/s/ms, ref. C_2H_4	3.2 ± 0.2[d]	11
H_2-d/f/ms	3.8 ± 0.2	20
H_2-Hgfp/sf/Lα	4.0 ± 0.1	this work
	D + CH_3SiH_3	
C_2D_4-p/s/ref. C_2D_4	2.7 ± 0.6[e]	7
D_2-d/f/ms	3.0 ± 0.8	9
D_2-d/f/ms	3.5 ± 0.4	20
	H + CH_3SiD_3	
H_2-Hgp/s/ms, ref. C_2H_4	1.2 ± 0.1[d]	11
	H + $(CH_3)_2SiH_2$	
H_2-Hgp/s/Lα, ref. C_2H_2	11 ± 3[c]	6
H_2-d/f/ms	4.1 ± 0.9	9
H_2-Hgp/s/ms, ref. C_2H_4	3.4 ± 0.4[d]	11
H_2-d/f/ms	2.8 ± 0.2	20
H_2-Hgfp/sf/Lα	3.1 ± 0.1	this work
	D + $(CH_3)_2SiH_2$	
C_2D_4-p/s/ref. C_2D_4	2.6 ± 0.6[e]	7
D_2-d/f/ms	1.4 ± 0.2	9
D_2-d/f/ms	2.2 ± 0.2	20
	H + $(CH_3)_3SiH$	
H_2-Hgp/s/Lα, ref. C_2H_2	10 ± 3[c]	6
H_2-d/f/ms	3.7 ± 1.0	9
H_2-Hgp/s/ms, ref. C_2H_4	3.0 ± 0.3[d]	11
H_2-Hgfp/sf/Lα	2.6 ± 0.1	this work

Table 2. (*continued*)

experimental system[b]	$k/10^{-13}$ cm^3 s^{-1}	ref.
	$D + (CH_3)_3SiH$	
C_2D_4-p/s/ref. C_2D_4	2.0 ± 0.5[c]	7
D_2-d/f/ms	1.7 ± 0.2	9
D_2-d/f/esr	3.3 ± 1.2[f]	12
D_2-d/f/ms	1.4 ± 0.2	20
	$H + (CH_3)_3SiD$	
H_2-d/f/ms	0.9 ± 0.1	18
H_2-Hgfp/sf/Lα	0.66 ± 0.02	this work
	$D + (CH_3)_3SiD$	
D_2-Hgfp/sf/Lα	0.84 ± 0.26[d]	19
	$H + C_2H_5SiH_3$	
H_2-Hgp/s/ms, ref. C_2H_4	3.9 ± 0.4[d]	11
	$H + (C_2H_5)_2SiH_2$	
H_2-Hgp/s/ms, ref. C_2H_4	6.6 ± 1.0[d]	11
	$H + (C_2H_5)_3SiH$	
H_2-Hgp/s/ms, ref. C_2H_4	5.3 ± 0.6[d]	11
H_2-Hgfp/sf/Lα	3.1 ± 0.3	this work
	$H + SiH_3Cl$	
H_2-Hgfp/sf/Lα	1.7 ± 0.1	this work
	$H + SiH_2Cl_2$	
H_2-Hgfp/sf/Lα	1.1 ± 0.1	this work
	$H + SiHCl_3$	
H_2-Hgfp/sf/Lα	0.53 ± 0.04	this work
	$H + SiHF_3$	
H_2-Hgfp/sf/Lα	<0.01	this work
	$H + C_6H_5SiH_3$	
H_2-Hgfp/sf/Lα	4.9 ± 0.2	this work
	$H + Si_2H_6$	
Si_2H_6-Hgp/s/ref. C_2H_4	19[d]	8
H_2-Hgp/s/ms, ref. C_2H_4	19.4 ± 1.3[d]	11
H_2-Hgfp/sf/Lα	14.5 ± 7.8	22
H_2-Hgfp/sf/Lα	12.9 ± 1.8	22[g]
	$D + Si_2H_6$	
C_2D_4-p/s/ref. C_2D_4	29 ± 9[e,h]	7
	$H + (CH_3)_3SiSi(CH_3)_2H$	
H_2-Hgfp/sf/Lα	10.0 ± 5.0	22
	10.3 ± 0.4	22[g]

[a] 295–305 K. [b] The following abbreviations are used: Hg, Hg photosensitized decomposition; d, microwave discharge; p, photolysis; fp, flash photolysis; pr, pulse radiolysis; s, static; f, flow; sf, quasistatic; Lα, Lyman-α; ms, mass spectrometry; esr, electron spin resonance; ref. X, reference reaction. [c] Normalized to $k(H + C_2H_2) = 2.08 \times 10^{-13}$ cm^3 s^{-1},[40] scaled to $k(H + C_2H_4)$ given in footnote *d*. [d] Normalized to $k(H + C_2H_4) = 6.3 \times 10^{-13}$ cm^3 s^{-1}, this work. [e] Normalized to $k(D + C_2D_4) = 4.63 \times 10^{-13}$ cm^3 s^{-1},[40] scaled to $k(H + C_2H_4)$ given in footnote *d*. [f] Re-evaluated from the original data. [g] Corrected to zero absorbed light intensity. [h] Evaluated *via* $k_{sub}/k_{abs} = 0.27 \pm 0.04$.[22]

calculated from $E_a(10)$, to compute a k^1 value at each temperature; $E_a(10)$ was varied until a good fit with the experimental k^1 values was obtained.

It can be seen from this account that the dependence of k_w on temperature had to be known. This was determined by measuring k_w at various temperatures, and the results were fitted to the power series, $k_w = a + b(T - 295\ \mathrm{K}) + c(T - 295\ \mathrm{K})^2$. In some cases it was found that the presence of the substrate appeared to alter the wall constant, resulting in k_w at room temperature being different from the value indicated by the intercept of plots of the kind shown in fig. 7. This was taken into account by adjusting the value of a to the value of k_w given by the plot.

The results obtained in this work are presented in table 1. The rate constants listed are those determined from the room-temperature measurements of k_0^1, E_a refers to the experimental activation energy, and $(E_a)_0$ to the activation energy corrected to zero intensity as described above. A_0 factors were calculated by combining the tabulated room-temperaure rate constants k_0 with the corresponding values of $(E_a)_0$. The error limits refer to one standard deviation and correspond to precision only. Also included in table 1 are results for Si_2H_6 and $(CH_3)_5Si_2H$, uncorrected Arrhenius parameters for which we reported previously.[22]

Reaction of H Atoms with C_2H_4

The addition of H atoms to C_2H_4 was used as a test reaction for the following reasons: its Arrhenius parameters are similar to those reported in this paper for the reactions of silanes; it has been employed as a reference reaction in a number of studies of hydrogen abstraction from silanes by H atoms; and it has recently been thoroughly studied by Lightfoot and Pilling.[34]

In our work, the pseudo-first-order rate constant showed a similar dependence on light intensity to that shown in fig. 6. Plotting the extrapolated zero-intensity rate constants against the C_2H_4 concentration gave $k_0 = (6.3 \pm 0.4) \times 10^{-13}\ \mathrm{cm^3\ s^{-1}}$ at 296 K. This value, which is slightly smaller than the high-pressure limiting rate constant given in ref. (34), has been used in table 2 to set the relative rate constants given in the literature on an absolute basis. The measured activation energy was given by $E_a/R = 870 \pm 70$ K. A computer simulation utilizing a mechanism similar to that in ref. (34) yielded $(E_a/R)_0 = 1050 \pm 85$ K.

Discussion

Rate Constants and Arrhenius Parameters

Reactivity Trends

As can be seen from tables 1 and 2, with the exception of SiF_3H, silanes show a high degree of reactivity towards H atoms. Earlier studies have shown that attack on the methyl groups does not occur, the only reaction being attack on the Si—H bond.[1] In the case of the disilanes, in addition to hydrogen abstraction, substitution is also observed.[8,21,22]

The main factor contributing to this preference for reaction at the silyl group is the low value of the Si—H bond dissociation energy, which also shows little variation with substitution at the Si atom. On average, this value is *ca.* 375 kJ $\mathrm{mol^{-1}}$,[35] which is lower than the bond dissociation energies of both the C—H and Si—Cl bonds, which are typically around 410[36] and 460 kJ $\mathrm{mol^{-1}}$,[35] respectively.

Neglecting the disilanes for the moment, we see that substitution of the H atoms in SiH_4 results in only a modest variation in the rate constant for H-atom attack. Again this follows from the small effect of substitution on the Si—H bond dissociation energy. If the results are scrutinized more closely, however, some trends can be discerned. One

pattern which emerges is that Cl substitution leads to lower rate constants than methyl substitution. It might be thought that this could be explained in terms of the inductive effect of the substituent on the Si—H bond-dissociation energy: a substituent exerting a $-I$ effect, like F or Cl, withdraws electrons from the Si—H bond, enhancing its polarity and hence increasing its bond-dissociation energy; this might be expected to lead to an increase in the activation energy for H-atom attack, and thus to a decrease in the rate constant. The opposite would be true for electron-donating groups like the methyl group. This explanation is certainly plausible for SiF_3H; the picture is less clear for the chlorosilanes, and fails for the methylsilanes, since within experimental error methyl substitution has no effect on the activation energy.

In the case of the chlorosilanes there is a slight increase in the activation energy along the series from SiH_4 to SiH_2Cl_2; only $SiCl_3H$ spoils the pattern, and this could possibly be due to interference by impurities, which are difficult to exclude from chlorosilanes. However, the room-temperature rate constants, the most reliable parameters determined in this work, are virtually the same when corrected for reaction-path degeneracy, leading to the conclusion that replacement of H by Cl has no noticeable effect.

Successive methyl substitution leads to an increase in the rate constant corrected for reaction-path degeneracy from $k/n = 0.5 \times 10^{-13}$ cm^3 s^{-1} for SiH_4 to 2.6×10^{-13} cm^3 s^{-1} for $(CH_3)_3SiH$, where n is the number of substrate Si—H bonds. Austin and Lampe[11] observed the same trend and they attributed it solely to changes in activation energy. In our case this would amount to a stepwise reduction of the activation temperature, E_a/R, from 1400 K for SiH_4 to 900 K for $(CH_3)_3SiH$. A look at table 1 assures us that this does not occur, and that the predominant contribution to the change in rate constant along the series is a corresponding change in A factor. This increase in A factor with methylation could be explained by two considerations related to the entropy of the transition state. With methyl substitution an increasing number of soft skeletal vibrations are introduced into the molecule, and if the frequencies of these vibrations suffer some reduction in the transition state an increase in A factor would result. A similar effect is achieved if the hindered internal rotation of the methyl groups becomes a free rotation in the transition state. The contribution of these internal rotors can be estimated with the help of the tables given by Pitzer and Gwinn.[37] If the barrier to rotation is taken to be 7.1 kJ mol^{-1},[38] the A factor for $(CH_3)_3SiH$ is calculated to be greater than that for SiH_4 by a factor of three. This is of the same magnitude as the observed value.

Replacing the methyl groups in $(CH_3)_3SiH$ by ethyl groups leads to a small increase in rate constant, mainly due to a slight decrease in activation energy.

The reaction of H atoms with $C_6H_5SiH_3$ was of interest because it offers the possibility of probing the magnitude of interaction between the radical centre and the phenyl ring. In the analogous carbon compound, toluene, this interaction leads to a considerable decrease in the C—H bond-dissociation energy. A smaller effect would be expected in the case of $C_6H_5SiH_3$ because of the poor overlap between the $3p_\pi$ and $2p_\pi$ orbitals of Si and C, and also because of the non-planarity of the molecule at the radical centre.[39] Our data show that this interaction is virtually non-existent, in agreement with results of Walsh.[35]

The two disilanes, Si_2H_6 and $(CH_3)_5Si_2H$, show the highest reactivity of all the substances investigated. Attack on these disilanes involves not only abstraction but also substitution, and therefore the rate constants given in table 1 must be apportioned accordingly. The substitution reaction, which involves a silyl group as the leaving group, is of considerable mechanistic interest, and has been dealt with in two previous publications.[21,22] The ratio of substitution to abstraction was found to be 0.27 ± 0.04 for Si_2H_6 and 0.164 ± 0.016 for $(CH_3)_5Si_2H$. Combining these values with the corresponding overall rate constants we obtain for the rate constants for hydrogen abstraction alone $(10.2 \pm 1.8) \times 10^{-12}$ cm^3 s^{-1} for Si_2H_6 and $(8.8 \pm 0.4) \times 10^{-13}$ cm^3 s^{-1} for $(CH_3)_5Si_2H$. On a per

Table 3. Arrhenius parameters for H- and D-atom attack on silanes and disilanes

reaction	E_a/kJ mol^{-1}	$A/10^{-11}$ cm^3 s^{-1}	ref.
$H+SiH_4$	11.6 ± 0.3	2.3 ± 0.3	this work
$D+SiH_4$	8.9 ± 0.8	0.73 ± 0.25	14
	10.5 ± 2.1	2.1 ± 2.0	15
$H+SiD_4$	10.4 ± 0.7	0.95 ± 0.29	14
	15.2 ± 0.7	4.2 ± 1.2	this work
$H+CH_3SiH_3$	10.1 ± 0.8	2.3 ± 0.9	20
	11.3 ± 0.7	4.0 ± 1.1	this work
$H+(CH_3)_2SiH_2$	11.7 ± 0.7	3.6 ± 1.1	this work
$H+(CH_3)_3SiH$	10.2 ± 0.6	1.7 ± 0.4	this work
$D+(CH_3)_3SiH$	11.0 ± 0.7	2.8 ± 0.5	12
$H+(CH_3)_3SiD$	13.4 ± 0.8	1.6 ± 0.6	this work
$D+(CH_3)_3SiD$	13.7 ± 1.0	2.1 ± 1.1	19[a]
$H+Si_2H_6$	9.6 ± 0.8	7.0 ± 3.0	22
	11.0 ± 0.9	11.6 ± 4.4	22[b]
$H+(CH_3)_3SiSi(CH_3)_2H$	8.0 ± 0.4	2.7 ± 0.7	22
	8.3 ± 0.4	3.0 ± 0.5	22[b]

[a] Activation energy corrected to zero absorbed light intensity by means of the ratio $(E_a/R)_0/(E_a/R)$ for $H+(CH_3)_3SiD$ from table 1; A factor obtained by combining corrected E_a value with k from table 2. [b] Corrected to zero absorbed light intensity.

Si—H basis, the rate constant for Si_2H_6 becomes 1.7×10^{-13} cm^3 s^{-1}. Thus replacing a hydrogen atom in SiH_4 by a silyl group has only a slightly larger effect than methyl substitution. The very high reactivity of the Si—H bond in $(CH_3)_5Si_2H$ stems mainly from its low activation energy. This may be an indication that the dissociation energy of the Si—H bond in the methyl-substituted disilanes is lower than that in the corresponding monosilanes.

Comparison with Previous Values

The rate constants obtained in this work are compared with previously published values in table 2, and the available Arrhenius parameters are listed in table 3. In several of the earlier studies, the rate of attack on the silane was compared with the rate of H- or D-atom addition to C_2H_4 or C_2D_4, and in one instance, to H-atom addition to C_2H_2. In order to put the comparison of the various results onto a common footing, we have recalculated rate constants and Arrhenius parameters from the original data on the basis of our parameters for $H+C_2H_4$, together with the ratios $k(H+C_2D_4)/k(H+C_2H_4)$ and $k(H+C_2H_2)/k(H+C_2H_4)$ from the recent paper by Sugawara *et al.*[40]

From table 2 it can be seen that, apart from several values which are clearly too high, there is general agreement between the results for SiH_4, and there is little difference between the rate constants for H- and D-atom attack. The pulse-radiolysis experiments of Mihelcic *et al.*[17] were carried out at high [H], under which conditions it would be expected that reaction (11) would be important. Hence, in order to compare their results with ours we have divided their published rate constant by two, and this is the value given in table 2. Mihelcic *et al.*[41] also measured a rate constant for $H+C_2H_4$ in their apparatus, and found the value $k=(1.25\pm0.03)\times10^{-12}$ cm^3 s^{-1}, twice that obtained in this work, thus providing further justification for our adjustment of their value. On this basis, our rate constant agrees well with the values of Austin and Lampe,[11] and Mihelcic *et al.*[17] for $H+SiH_4$, and with those of Mihelcic *et al.*[17] and Potzinger *et al.*[14] for $D+SiH_4$. The results of Wörsdorfer *et al.*[20] would almost certainly have been affected by the surface under the low-pressure conditions which obtained in their flow experiments,

and this may account for their value being higher than the other results from this laboratory. For $H+SiD_4$ there is again good agreement between the work done by this group and the rate constant of Austin and Lampe.[11]

A similarly consistent picture emerges from inspection of the methylsilane results: for H-atom attack, our rate constants agree well with those of Austin and Lampe,[11] and Wörsdorfer *et al.*,[20] and although the data available for D-atom attack are less reliable than those for H-atom attack, it appears that, as for SiH_4, there is little to choose between the results for the H- and D-atom reactions. There is closer agreement between our results and those of Wörsdorfer *et al.*[20] for the methylsilanes than for SiH_4; this is consistent with the lower surface activity exhibited by methylsilanes compared with SiH_4. The rate constant reported by Ellul *et al.*[19] for $D+(CH_3)_3SiD$ was measured in an earlier version of our apparatus before the characteristic dependence of k^1 on I_{abs} had been fully appreciated. Ellul *et al.* also measured a rate constant for $H+C_2H_4$, and obtained $k=(1.2\pm0.2)\times10^{-12}$ cm^3 s^{-1}. This value is, as expected, nearly twice the extrapolated zero intensity value found in the present instance, and we have therefore adjusted their rate constant for $D+(CH_3)_3SiD$ accordingly. The adjusted value is nearly the same as that obtained in our work on $H+(CH_3)_3SiD$.

The only Arrhenius parameters for $H+SiH_4$ are those reported here, but for $D+SiH_4$, Arrhenius parameters have been determined in this laboratory by Potzinger *et al.*[14] and Mihelcic *et al.*[15] From table 3 it can be seen that the results of the former are noticeably lower than those of the latter. Since Potzinger *et al.* carried out their experiments at low temperatures (144–298 K), this behaviour could be rationalized in terms of quantum-mechanical tunnelling. A similar pattern is apparent in the Arrhenius parameters for $H+SiD_4$, where the values of Potzinger *et al.*[14] are significantly lower than those found in this work. Comparison of our parameters for $H+SiH_4$ with those of Mihelcic *et al.*[15] for $D+SiH_4$ shows that both the A factors and activation energies are equal within experimental error.

In addition to those reported here, Arrhenius parameters for attack on the methylsilanes have been determined in this laboratory by Wörsdorfer *et al.*[20] for $H+CH_3SiH_3$, and by Contineanu *et al.*[12] for $D+(CH_3)_3SiH$. Again the values for each reaction agree within experimental error.

The rate constant of Fabry *et al.*[22] for $H+Si_2H_6$, corrected to zero intensity, is lower than those of Pollock *et al.*[8] and Austin and Lampe,[11] and much lower than that of Obi *et al.*[7] for $D+Si_2H_6$. The reliability of the results of Obi *et al.* is in some doubt, however, since Si_2H_6 absorbs strongly at $\lambda > 210$ nm, and therefore some may have been photolysed by the iodine lamp (which emits in the range 170–206 nm) which was used in their experiments for the photolysis of C_2D_4.

Kinetic Isotope Effects

From the results in tables 2 and 3, kinetic isotope effects, k_H/k_D, can be evaluated, and these are given in table 4. Also included are A factor ratios, A_H/A_D, and activation energy differences, $E_{aD}-E_{aH}$, where the corresponding Arrhenius parameters were available. Some of the values shown were obtained by combining results from different studies, and they should therefore not be considered as reliable as those deduced from rate constants measured in the same apparatus.

From transition-state theory it can be shown that the upper limit of the kinetic isotope effect for abstraction from X—H/X—D bonds is given by $k_H/k_D=\exp(\Delta E_{zp})/RT$, where ΔE_{zp} is the difference in zero-point energies of the X—H and X—D bonds. Thus, $E_{aD}-E_{aH}=\Delta E_{zp}$ and $A_H/A_D=1$. In the case of SiH_4/SiD_4, since $\omega(Si—H)=2187$ cm^{-1} and $\omega(Si—D)=1558$ cm^{-1},[42] $\Delta E_{zp}=3.76$ kJ mol^{-1}, which gives $k_H/k_D=4.6$ at 298 K. Similar frequencies are found for the methylsilanes[43] and hence similar values for the kinetic isotope effect are predicted.

Table 4. Kinetic isotope effects for H- and D-atom attack on silanes and disilanes

reaction	k_H/k_D	$E_{aD}-E_{aH}$/kJ mol^{-1}	A_H/A_D	ref.
$H/D+SiH_4$	1.3 ± 0.3			17
	1.1 ± 0.3			20
$H+SiH_4/SiD_4$	2.8 ± 0.5			11
	2.4 ± 0.2	3.6 ± 0.8	0.55 ± 0.17	this work
$H/D+CH_3SiH_3$	1.1 ± 0.1			20
$H+CH_3SiH_3/CH_3SiD_3$	2.7 ± 0.3			11
$H/D+(CH_3)_2SiH_2$	1.3 ± 0.1			20
$H/D+(CH_3)_3SiH$	0.79 ± 0.29	0.78 ± 0.91	0.61 ± 0.27	this work, 12
	1.9 ± 0.3			this work, 20
$H/D+(CH_3)_3SiD$	0.79 ± 0.24	0.3 ± 1.3	0.76 ± 0.49	this work, 19
$H+(CH_3)_3SiH/(CH_3)_3SiD$	3.9 ± 0.2	3.2 ± 1.0	1.1 ± 0.5	this work
$D+(CH_3)_3SiH/(CH_3)_3SiD$	3.9 ± 1.9	2.7 ± 1.2	1.3 ± 0.7	12, 19
	1.7 ± 0.6			20, 19
$H+Si_2H_6/Si_2D_6$	2.5 ± 0.2			11

A clear picture emerges from the results in table 4: substituting D for H as the attacking atom has little effect on the rate constant, while isotopic substitution at the Si—H bond of the substrate leads to a large kinetic isotope effect, close to the upper limit value indicated by transition-state theory. This seems to imply that these reactions proceed *via* a 'late' transition state, behaviour which runs counter to that predicted by Hammond's principle,[44] according to which the transition state of an exothermic reaction should be located in the reactant valley of the potential-energy surface. We have also carried out BEBO[3,4] calculations on the simpler silane systems, and they too indicate that an early transition state is involved.

The apparent variance between expected and actual behaviour could be interpreted as an indication that H-atom abstraction from these silanes is not a direct process. It would be premature to come to this conclusion, however, especially since the same reactivity pattern is found in the $O+SiH_4/SiD_4$ system,[45] where it was shown that H-atom transfer is a direct process.[46] An appreciable contribution to the isotope effect could also come from tunnelling processes.

References

1 N. L. Arthur and T. N. Bell, *Rev. Chem. Intermed.*, 1978, **2**, 37.
2 J. A. Kerr and S. J. Moss, *CRC Handbook of Bimolecular and Termolecular Gas Reactions* (CRC Press, Boca Raton, 1981), vol. 1.
3 H. S. Johnston, *Gas Phase Reaction Rate Theory* (The Ronald Press Company, New York, 1966).
4 R. L. Brown, *J. Res. Natl. Bur. Stand. (U.S.)*, 1981, **86**, 605.
5 G. K. Moortgat, *Diss. Abstr. B*, 1970, **31**, 1879.
6 J.-H. Hong, *Ph.D. Thesis* (University of Detroit, 1972).
7 K. Obi, H. S. Sandhu, H. E. Gunning and O. P. Strausz, *J. Phys. Chem.*, 1972, **76**, 3911.
8 T. L. Pollock, H. S. Sandhu, A. Jodhan and O. P. Strausz, *J. Am. Chem. Soc.*, 1973, **95**, 1017.
9 J. A. Cowfer, K. P. Lynch and J. V. Michael, *J. Phys. Chem.*, 1975, **79**, 1139.
10 K. Y. Choo, P. P. Gaspar and A. P. Wolf, *J. Phys. Chem.*, 1975, **79**, 1752.
11 E. R. Austin and F. W. Lampe, *J. Phys. Chem.*, 1977, **81**, 1134.
12 M. A. Contineanu, D. Mihelcic, R. N. Schindler and P. Potzinger, *Ber. Bunsenges. Phys. Chem.*, 1971, **75**, 426.
13 L. C. Glasgow, G. Olbrich and P. Potzinger, *Chem. Phys. Lett.*, 1972, **14**, 466.
14 P. Potzinger, L. C. Glasgow and B. Reimann, *Z. Naturforsch., Teil A*, 1974, **29**, 493.
15 D. Mihelcic, P. Potzinger and R. N. Schindler, *Ber. Bunsenges. Phys. Chem.*, 1974, **78**, 82.
16 B. Reimann and P. Potzinger, *Ber. Bunsenges. Phys. Chem.*, 1976, **80**, 565.
17 D. Mihelcic, V. Schubert, R. N. Schindler and P. Potzinger, *J. Phys. Chem.*, 1977, **81**, 1543.
18 K. Wörsdorfer, *Ph.D. Thesis* (University of Essen, 1979).

19 R. Ellul, P. Potzinger, B. Reimann and P. Camilleri, *Ber. Bunsenges. Phys. Chem.*, 1981, **85**, 407.
20 K. Wörsdorfer, B. Reimann and P. Potzinger, *Z. Naturforsch., Teil A.* 1983, **38**, 896.
21 R. Ellul, P. Potzinger and B. Reimann, *J. Phys. Chem.*, 1984, **88**, 2793.
22 L. Fabry, P. Potzinger, B. Reimann, A. Ritter and H. P. Steenbergen, *Organomet.*, 1986, **5**, 1231.
23 R. A. Back, *Can. J. Chem.*, 1954, **37**, 1834.
24 G. R. De Maré, *J. Photochem.*, 1977, **7**, 101.
25 A. Lifshitz, G. B. Skinner and D. R. Wood, *Rev. Sci. Instr.*, 1978, **49**, 1322.
26 H. Okabe, *Photochemistry of Small Molecules* (Wiley-Interscience, New York, 1978).
27 A. C. G. Mitchell and M. W. Zemansky, *Resonance Radiation and Excited Atoms* (Cambridge University Press, Cambridge, 1971).
28 M. F. R. Mulcahy, *Gas Kinetics* (Nelson, London, 1973).
29 A. B. Callear and R. G. W. Norrish, *Proc. R. Soc. London, Ser. A*, 1962, **266**, 299; A. B. Callear and G. J. Williams, *Trans. Faraday Soc.*, 1964, **60**, 2158; A. B. Callear and R. E. M. Hedges, *Trans. Faraday Soc.*, 1970, **66**, 605; A. B. Callear and R. E. M. Hedges, *Trans. Faraday Soc.*, 1970, **66**, 615; A. B. Callear and J. C. McGurk, *J. Chem. Soc., Faraday Trans. 2*, 1972, **68**, 289; A. B. Callear and P. M. Wood, *J. Chem. Soc., Faraday Trans. 2*, 1972, **68**, 302; A. B. Callear and J. C. McGurk, *J. Chem. Soc., Faraday Trans. 2*, 1973, **69**, 97. K. Oka and R. J. Cvetanovic, *J. Chem. Phys.*, 1978, **68**, 4391; D. Wyrsch, H. R. Wendt and H. E. Hunziker, *Ber. Bunsenges. Phys. Chem.*, 1974, **78**, 204.
30 H. A. Bethe and E. E. Salpeter, *Handbuch der Physik Vol.* XXXV, Springer 1957.
31 A. Stock and C. Somieski, *Berichte*, 1919, **52**, 719.
32 H. S. Booth and W. D. Stillwell, *J. Am. Chem. Soc.*, 1934, **56**, 1529.
33 W. L. Jolly, *Inorg. Synth.*, 1968, **11**, 170.
34 P. D. Lightfoot and M. J. Pilling, *J. Phys. Chem.*, 1987, **91**, 3373.
35 R. Walsh, *Acc. Chem. Res.*, 1981, **14**, 246.
36 D. F. McMillen and D. M. Golden, *Annu. Rev. Phys. Chem.*, 1982, **33**, 493.
37 K. S. Pitzer and W. D. Gwinn, *J. Chem. Phys.*, 1942, **10**, 428.
38 L. Pierce and D. H. Petersen, *J. Chem. Phys.*, 1960, **33**, 907.
39 P. J. Krusic and J. K. Kochi, *J. Am. Chem. Soc.*, 1969, **91**, 3938.
40 K. Sugawara, K. Okazaki and S. Sato, *Bull. Chem. Soc. Jpn*, 1981, **54**, 2872.
41 D. Mihelcic, V. Schubert, F. Höfler and P. Potzinger, *Ber. Bunsenges. Phys. Chem.*, 1975, **79**, 1230.
42 T. Shimanouchi, *Tables of Molecular Vibrational Frequencies*, Consolidated Volume 1, 1972, NSRDS-NBS 39.
43 J. L. Duncan, *Spectrochim. Acta*, 1964, **20**, 1807.
44 G. C. Hammond, *J. Am. Chem. Soc.*, 1955, **77**, 334.
45 R. Taege, O. Horie, P. Potzinger and B. Reimann, to be published.
46 B. S. Agrawalla and D. W. Setser, *J. Chem. Phys.*, 1987, **86**, 5421.

Paper 8/04677K; *Received* 25*th November*, 1988